Sign-Engineered Interactions Enable Dynamic Frustration and Topology in a Passive Elastic Lattice

Taehwa Lee,[a] Ziqi Yu[1], Xiaoshi Su[1], Hyung-Suk Kwon[1], and Chiara Daraio[2][b]

CONTENTS

---

[a] Electronic mail: taehwa.lee@toyota.com
[b] Electronic mail: daraio@caltech.edu

I. SUPPLEMENTARY FIGURES

A. Extraction of effective coupling strength and sign from H

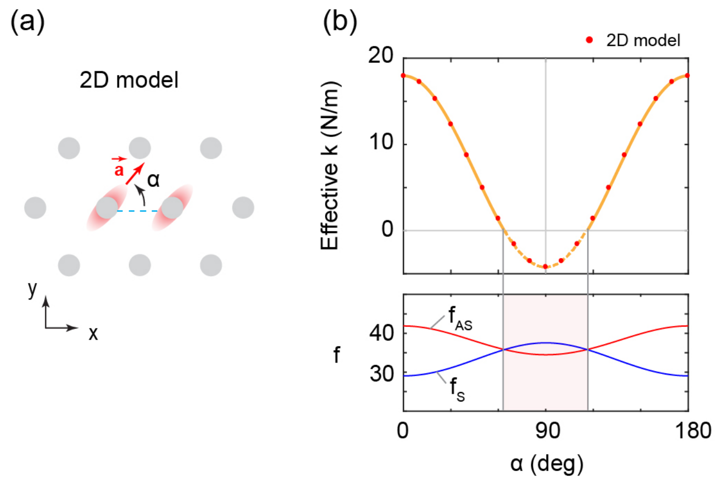

Figure S1. Extraction of coupling strength and sign in a two-mass system. (a) 2D model used to extract coupling strength and sign. Two masses with local anisotropy are surrounded by fixed atoms. (b) Comparison of the effective coupling (Eq.(3), solid) with that calculated from the two-mass 2D model (symbol). In the 2D model, antisymmetric (f_{AS}) and symmetric (f_{S}) mode frequencies are used to calculate coupling strengths, $k_{\mathrm{eff}} = m/2(\omega_{\mathrm{AS}}^2 - \omega_{\mathrm{S}}^2)$ with $\omega_{\mathrm{S(AS)}} = 2\pi f_{\mathrm{S(AS)}}$.

B. Separation of a- and b-manifolds

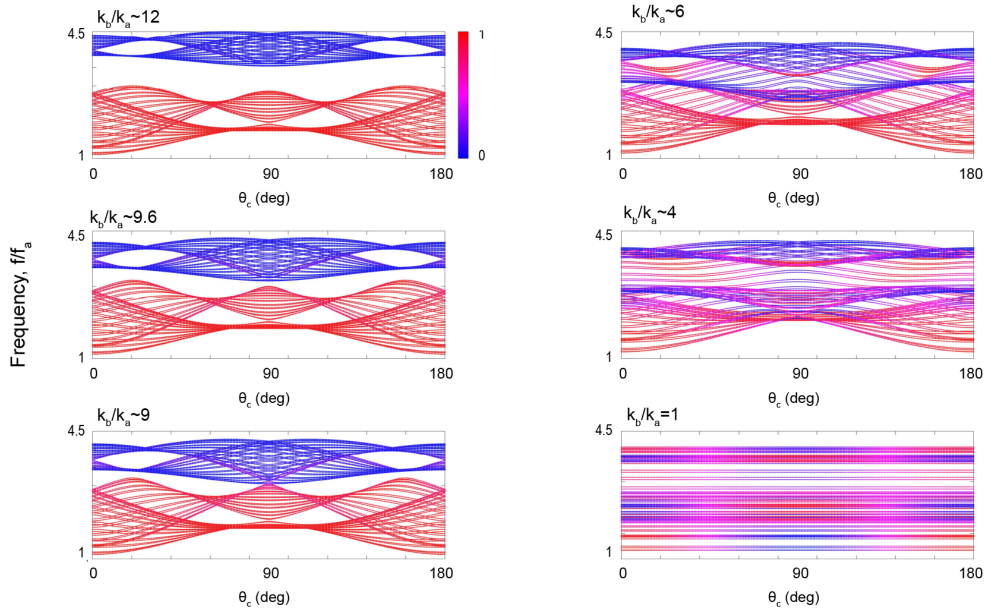

Figure S2. Manifold separation. Frequency bands for varying k_b/k_a. k_b/k_a 9.6 exhibits clear separation of the frequency bands, but $P_a \neq 0, 1$. $k_b/k_a < 9$ induces mode mixing.

C. Phase Diagrams: Nonlocal, dimerization, and frustrated regimes

The nonlocality $L(\theta_c)$ is characterized by

$$L(\theta_c) = \frac{|k_{\rm LR}|}{\max(k_{\rm inter}, k_{\rm intra})},$$

ranging from 0 to 1.

The dimerization $D(\theta_c)$, enabled by $k_{\rm inter} \neq k_{\rm intra}$ while greater than $k_{\rm LR}$, is characterized by

$$D(\theta_c) = \frac{|k_{\rm inter}| - |k_{\rm intra}}{k_{\parallel}},$$

ranging from -1 ($k_{\rm inter} < k_{\rm intra}$) to 1 ($k_{\rm inter} > k_{\rm intra}$).

The frustration $F(\theta_c)$ is characterized by

$$F(\theta_c) = -\frac{\mathrm{sign}(k_{\rm inter}\, k_{\rm intra}\, k_{\rm LR})\, |k_{\rm inter}\, k_{\rm intra}\, k_{\rm LR}|^{1/3}}{(|k_{\rm inter}| + |k_{\rm intra}| + |k_{\rm LR}|)\,/3},$$

ranging from 0 (ordinary) to 1 (frustration).

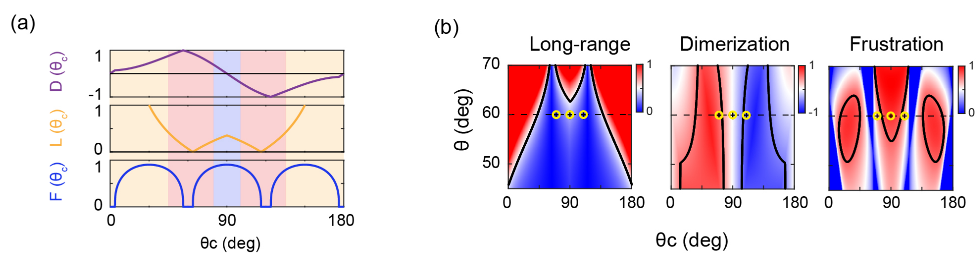

Figure S3. Phase diagrams. (a) Dimerization $D(\theta_c)$, nonlocality $L(\theta_c)$, and frustration $F(\theta_c)$ for angles between bonds ($\theta = 60°$). Color shades indicate dominant regimes (yellow for nonlocality, red for dimerization, and blue for frustration). (b) Corresponding D, L, F for varying θ while keeping the same length (d) along the zigzag bonds (LR bond length $l = 2d\cos\theta$). The horizontal dashed line indicates $\theta = 60°$ with three representative anisotropy angles $\theta_c = 70°, 90°, 110°$.

D. Topological edge mode (both in a- and b-manifolds)

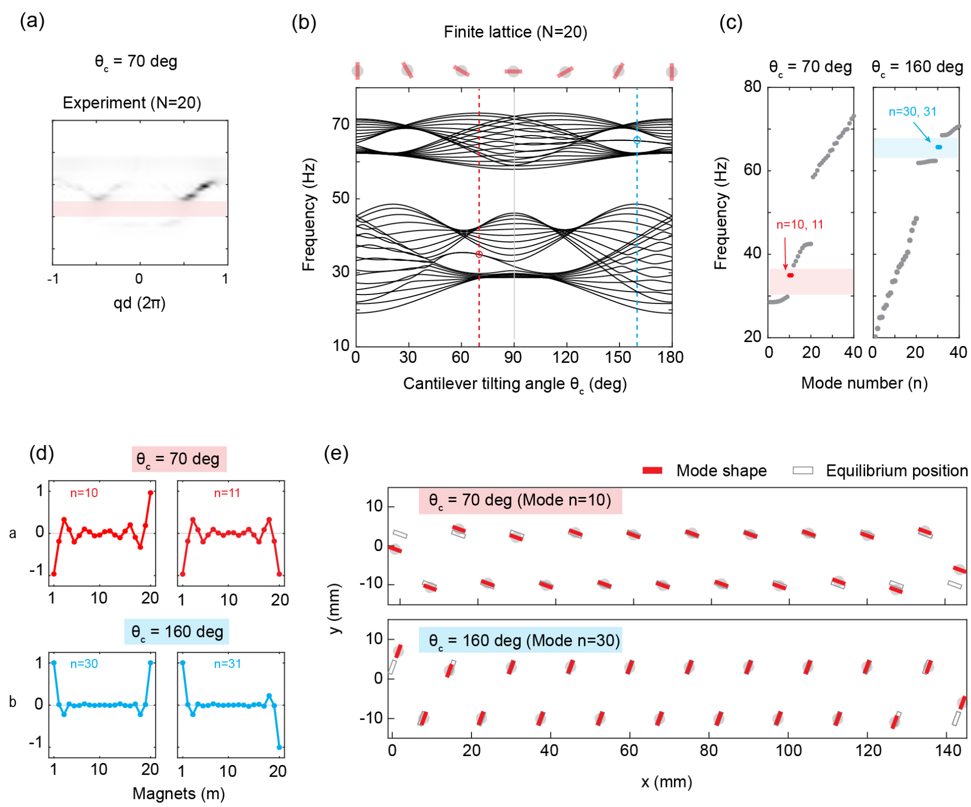

Figure S4. Topological phase. (a) Measured dispersion relation of the lattice of $\theta_c = 70°$ with the bandgap highlighted by the red shade. (b) Modes (a- and b-manifolds) for the finite lattice ($N = 20$). Topological edge modes for $\theta_c = 40° - 90°$ in a-manifold and for $\theta_c = 130° - 180°$. (c) Modes for $\theta_c = 70°, 160°$. (d) Topological edge modes ($n = 10, 11$ in a-manifold) for $\theta_c = 70°$ and topological edge modes ($n = 30, 31$ in b-manifold) for $\theta_c = 160°$. (e) Mode shapes for $n = 10$ ($\theta_c = 70°$) and $n = 30$ ($\theta_c = 160°$).

E. Nonlocality

Correlation between rows, $C(f)$ is characterized by

$$C(f) = \frac{\sum_m u_{\mathrm{top}}(m)\, u_{\mathrm{bot}}(m)}{\sqrt{\sum_m u_{\mathrm{top}}^2(m) \;\; \sum_m u_{\mathrm{bot}}^2(m)}},$$

with $u_{\mathrm{top(bot)}}$ being the displacements of top (bottom) row.

$$\begin{cases} C \approx +1 & : \text{symmetric (in-phase)}, \\ C \approx -1 & : \text{antisymmetric (out-of-phase)} \end{cases}$$

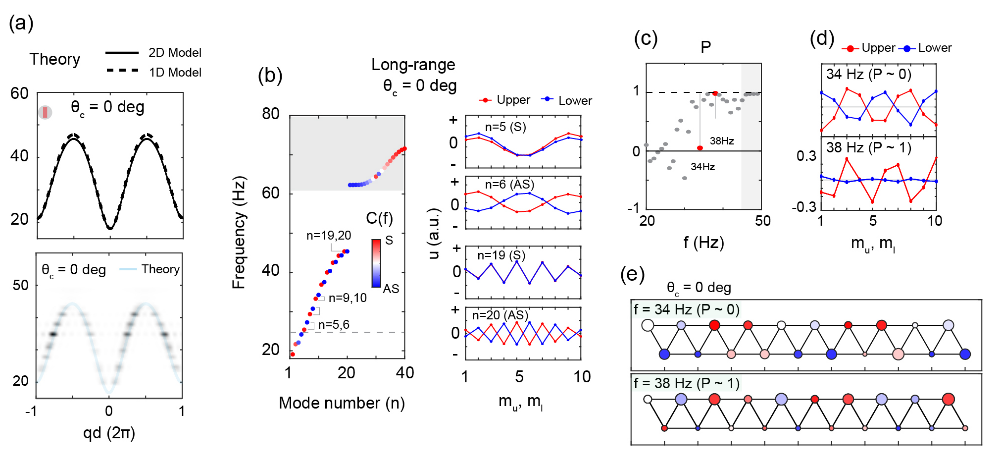

Figure S5. Different regimes. (a) Dispersion relations (a-manifold) for theory (top) and experiment (bottom) at $\theta_c = 0°$. (b) Corresponding modes: modes in lower bands correspond to nonlocality. Color indicates correlation between top and bottom rows $C(f)$ ($C = 1$ symmetric and $C = -1$ antisymmetric). Mode profiles plotted separately for top and bottom rows. (c) P calculated for the measured displacement. $P = 0$ at 34 Hz and $P = 1$ at 38 Hz. (d) Measured antisymmetric profiles at 34 Hz ($P = 0$) and Top row polarized at 38 Hz ($P = 1$). (e) Corresponding phase and amplitude diagrams.

F. Experimental setup

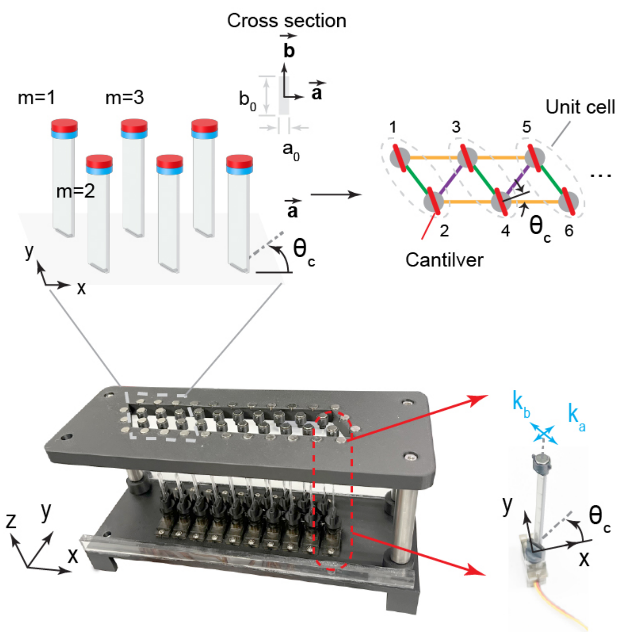

Figure S6. Experimental setup. Photo of the fabricated device.

II. SUPPLEMENTARY VIDEOS

Video 1. High-speed imaging for anisotropy angle $\theta_c = 90^\circ$ frustration at 27 Hz

Video 2. High-speed imaging for anisotropy angle $\theta_c = 90^\circ$ unfrustrated at 34 Hz

Video 3. High-speed imaging for anisotropy angle $\theta_c = 70^\circ$ topological edge mode at 33 Hz

Video 4. High-speed imaging for anisotropy angle $\theta_c = 70^\circ$ bulk mode at 38 Hz

Video 5. High-speed imaging for anisotropy angle $\theta_c = 0^\circ$ nonlocal mode at 38 Hz